

## A Linkage Observed between Austral Autumn Antarctic Oscillation and Preceding Southern Ocean SST Anomalies

CHUNDI HU

*School of Atmospheric Sciences, Nanjing University, Nanjing, Jiangsu, and Institute of Earth Climate and Environment System, Sun Yat-sen University, Guangzhou, Guangdong, China*

QIGANG WU

*School of Atmospheric Sciences, Nanjing University, Nanjing, Jiangsu, China*

SONG YANG

*School of Atmospheric Sciences, and Institute of Earth Climate and Environment System, Sun Yat-sen University, Guangzhou, Guangdong, China*

YONGHONG YAO AND DUO CHAN

*School of Atmospheric Sciences, Nanjing University, Nanjing, Jiangsu, China*

ZHENNING LI AND KAIQIANG DENG

*School of Atmospheric Sciences, and Institute of Earth Climate and Environment System, Sun Yat-sen University, Guangzhou, Guangdong, China*

(Manuscript received 6 June 2015, in final form 15 January 2016)

### ABSTRACT

In this study, the authors apply a lagged maximum covariance analysis (MCA) to capture the cross-seasonal coupled patterns between the Southern Ocean sea surface temperature (SOSST) and extratropical 500-hPa geopotential height anomalies in the Southern Hemisphere, from which Niño-3.4 signals and their linear trends are removed to a certain extent. Statistically significant results show that the dominant feature of ocean–atmosphere interaction is likely the effect of atmosphere on SOSST anomalies, with a peak occurring when the atmosphere leads the SOSST by 1 month.

However, the most eye-capturing phenomenon is that the austral autumn atmospheric signal, characterized by a negatively polarized Antarctic Oscillation (AAO), is significantly related to the gradual evolution of preceding SOSST anomalies, suggesting that the SOSST anomalies tend to exert an effect on the Southern Hemisphere atmospheric circulation. A regression analysis based on SOSST anomaly centers confirms these features. It is also demonstrated that the gradual evolution of changes in SOSST is mainly driven by internal atmospheric variability via surface turbulent heat flux associated with cold or warm advection and that the atmospheric circulation experiences a change from a typical positive AAO to a negative phase in this process. These findings indicate that such a long lead cross-seasonal covariance could contribute to a successful prediction of AAO-related atmospheric circulation in austral autumn from the perspective of SOSST anomalies, with lead times up to 6–7 months.

### 1. Introduction

There is a growing effort to predict the atmospheric circulation on seasonal-to-interannual time scales related to extratropical ocean–atmosphere interaction

*Corresponding author address:* Prof. Qigang Wu, School of Atmospheric Sciences, Nanjing University, Xianlin Campus, 163 Xianlin Boulevard, Nanjing, Jiangsu 210023, China.

E-mail: qigangwu@nju.edu.cn; yangsong3@mail.sysu.edu.cn

[see review by [Kushnir et al. \(2002\)](#)]. In the Southern Hemisphere (SH), the Antarctic Oscillation (AAO, also called the southern annular mode; [Gong and Wang 1999](#)) is the leading mode of the empirical orthogonal function (EOF) analysis based on the month-to-month sea level pressure (SLP) or geopotential height south of 20°S, which explains 20%–30% of the total variability ([Thompson and Wallace 2000](#); [Sen Gupta and England 2007](#)). It is characterized as an zonally quasi-symmetric

pattern that spans all longitudes between high latitudes (poleward of 50°S) and middle latitudes (30°–50°S), with an equivalent barotropic structure in the vertical (e.g., Kidson 1988; Karoly 1989; Thompson and Wallace 2000; Lorenz and Hartmann 2001; Wu and Zhang 2011). Both model experiments and observational studies have shown that the existence of AAO results from the meridional shift or swing in the position of the transient eddy-driven westerly jet stream that is typically located near 50°S (e.g., Hartmann and Lo 1998; Limpasuvan and Hartmann 2000; Lorenz and Hartmann 2001; Codron 2005, 2007; Wang et al. 2015).

The influence of AAO, however, not only is accompanied by climate anomalies in the SH (e.g., Hall and Visbeck 2002; Gillett et al. 2006; Ciasto and Thompson 2008; Sen Gupta and England 2007; Wang et al. 2015), but also extends well into the Northern Hemisphere (NH). For example, a strong AAO in boreal spring is usually accompanied by a weakened East Asian summer monsoon, a strengthened and westward expanded western Pacific subtropical high, and enhanced summer precipitation over the Yangtze River valley (Nan and Li 2003; Xue et al. 2003; Nan et al. 2009), suggesting that the AAO is another valuable precursory signal for the summer rainfall over East Asia apart from El Niño–Southern Oscillation (ENSO). Zheng et al. (2015) demonstrated that the boreal spring AAO could influence the summer air temperature over northeast China. Fan and Wang (2004, 2006) revealed that the boreal winter–spring AAO was negatively correlated with the frequency of spring dust storms in northern China. Zheng and Li (2012) suggested that boreal winters with a strong positive AAO were often followed by less spring [March–May (MAM)] rainfall over South China, and vice versa. Furthermore, Yue and Wang (2008) found a significant positive correlation between boreal winter AAO and the following spring North Asian cyclone activity. The AAO also exerts great influences on the East Asian winter monsoon (Wu et al. 2009), the North American summer monsoon (Sun 2010), and the West African summer monsoon (Sun et al. 2010). In spite of the obvious potential benefits of AAO for skillful seasonal prediction of NH climate, however, only little attention has been paid to the predictability and prediction of seasonal AAO variations (Lim et al. 2013).

Previous studies have shown that the AAO exerts a significant impact on the underlying sea surface temperature (SST) or sea ice concentration (SIC) (e.g., Hall and Visbeck 2002; Lovenduski and Gruber 2005; Verdy et al. 2006; Sen Gupta and England 2006, 2007; Ciasto and Thompson 2008; Wu and Zhang 2011; Wang et al. 2015). Anomalous patterns of SST/SIC associated with the AAO vary with seasons and are largely generated via changes in anomalous surface turbulent heat fluxes, and to a less extent the Ekman transport (Sen Gupta and

England 2007; Ciasto and Thompson 2008). On the other hand, there exists also evidence of feedback from the Southern Ocean SST (SOSST) onto the overlying atmospheric circulations (e.g., Raphael 2003; Lachlan-Cope 2005; Marshall and Connolley 2006; Sen Gupta and England 2006, 2007), although the amplitude of atmospheric response is relatively weaker than the intrinsic atmospheric variability (Watterson 2001; Raphael and Holland 2006; Sen Gupta and England 2007). The feedback of SST/SIC anomalies on the overlying atmospheric circulation involves nonadiabatic heating that is due mainly to the changes in surface heat flux and transient eddy flux.

According to Wu and Zhang (2011), statistically significant cross-seasonal covariance can be found between austral spring AAO and preceding Antarctic dipole-like SIC anomalies up to 4 months earlier, and the relationship is independent of ENSO signals. Relative to the Antarctic SIC anomalies, however, few studies have forecast the exact season and time period of the atmospheric links to preceding SOSST anomalies. The current study is aimed at investigating whether there exists any linear covariability between preceding SOSST anomalies and SH extratropical atmospheric circulation during certain seasons. Motivated by Wu and Zhang (2010, 2011), we examine the potential atmospheric linkage to SOSST anomalies as a function of monthly time lag by using a lagged maximum covariance analysis (MCA). The lagged MCA analysis is an excellent climate analysis method, which has been widely used for identifying the potential links of atmospheric signals to external forcing (e.g., Czaja and Frankignoul 1999, 2002; Wen et al. 2005; Liu et al. 2006; Frankignoul and Sennéchal 2007; Wu 2008, 2010; Wu and Zhang 2010, 2011; Wu et al. 2011).

On seasonal to interannual time scales, the atmosphere primarily acts as a “white noise” forcing on extratropical ocean to generate a “red noise” SST response. In this respect, if the SOSST only responds passively, there should be no significant cross-seasonal covariance in the lagged MCA between prior SOSST anomalies and later SH atmospheric variations beyond the atmospheric persistence. However, if the SOSST anomalies exert a substantial impact on the SH atmosphere, significant cross-seasonal covariance should exist when the SOSST lead time is longer than the atmospheric persistence time (Czaja and Frankignoul 2002). The current study seeks such signals by applying a lagged MCA between SOSST and SH Z500 anomalies to identify their cross-seasonal coupled patterns and discover their geographic origins. A significant atmospheric linkage during austral autumn to the preceding spring SOSST anomalies with lead time up to 6–7 months is reported.

The remainder of this paper is structured as follows. Section 2 describes the data sources and analysis techniques. Sections 3 and 4 present the main results obtained. A summary and discussion are provided in section 5.

## 2. Data and analysis methodology

Considering the better quality of data for the satellite era (Kistler et al. 2001; Renwick 2002) and the difference in mean climatic states related to the well-known “climate shift” in the mid-to-late 1970s (e.g., Trenberth and Hurrell 1994; Mantua et al. 1997; Nakamura et al. 1997; Wang et al. 2007, 2008, 2010), we use the monthly atmospheric data from the European Centre for Medium-Range Weather Forecasts interim reanalysis (ERA-Interim; Dee et al. 2011). The data used include sea level pressure; geopotential height at 925, 700, 500, and 200 hPa (Z925, Z700, Z500, and Z200); and winds and temperature at 925 hPa (T925 and UV925). The latent and sensible heat fluxes used are obtained from the Objectively Analyzed Air–Sea Fluxes (OAFlux) website (<http://oaflux.whoi.edu>), in which the OAFlux is constructed from an optimal blending of satellite retrievals and atmospheric reanalyses (Yu et al. 2004, 2006, 2008). The ensemble mean of two SST datasets, obtained from the NOAA Extended Reconstructed SST version 3b dataset (ERSSTv3b; Smith et al. 2008) and the Hadley Centre Global Sea Ice and Sea Surface Temperature (HadISST) analyses (Rayner et al. 2003), is used in this study. Here the HadISST dataset is interpolated to a regular  $2^\circ \times 2^\circ$  longitude/latitude grid as the ERSSTv3b. We compute the results over the 35-yr period of 1979–2013, and over the 30-yr period of 1979–2008 on account of the available data of OAFlux. The Niño-3.4 index is downloaded from <http://www.cpc.ncep.noaa.gov/data/indices/> and the AAO index is defined as the leading principal component of SH extratropical Z500 anomalies as in Thompson and Wallace (2000).

We apply the lagged MCA to capture the dominant coupled modes between Z500 ( $20^\circ\text{--}90^\circ\text{S}$ ) and SOSST ( $20^\circ\text{--}70^\circ\text{S}$ ), with an equal area weight at each grid point by multiplying the square root of the cosine of latitudes due to the decrease in area toward the pole (North et al. 1982a,b). Each set of successive 3-month seasons [e.g., January–March (JFM)] is considered with SOSST leading or lagging Z500. Note that the lagged MCA and other analyses used in this study are all performed with monthly data rather than seasonally averaged data (i.e., a JFM season has 3 months, and so the JFM seasons of 30 years have 90 months in total). The lagged MCA patterns describe the spatial structure of each respective field, and the corresponding squared singular values represent the squared covariance fraction (SCF), which

in turn reflects the relative importance of each MCA pattern in relation to the total covariance of two fields. To illustrate whether the lagged MCA results are meaningful, a Monte Carlo test (Shen and Lau 1995) is chosen to assess the statistical significance. The test is repeated 1000 times at each lag by using the original SOSST and randomly scrambled Z500 data. The so-called significance level indicates that the percentage of randomized squared covariance (SC), SCF, and temporal correlation (CORR) exceeds the one being tested.

Previous studies have revealed several important features. 1) There are different long-term trends of AAO during austral summer, autumn, and winter over the past decades (e.g., Thompson and Solomon 2002; Gillett and Thompson 2003; Marshall et al. 2004; Miller et al. 2006; Ding et al. 2011). 2) A Rossby wave train exists as a Pacific–South American teleconnection pattern, which is a typical remote response to ENSO signals (e.g., Karoly 1989; Cai and Baines 2001; White et al. 2002; Ding et al. 2012). 3) The skill of seasonal predictability of AAO is strongly associated with ENSO signals (Lim et al. 2013; Wang and Cai 2013). Therefore, to reduce the influences of long-term trends and ENSO forcing to a certain extent, we separately remove linear trends using the least squares method and filter out ENSO signals using a regression against the conventional ENSO index (Niño-3.4) for each month before applying the lagged MCA. Considering the delayed forcing of ENSO, the removal of ENSO signals from SOSST or Z500 should be a function of time (monthly lag) to obtain a more objective response (Frankignoul et al. 2014). Hence the regression coefficient for removing ENSO signals is chosen as the maximum within the preceding 6 months as in Liu et al. (2006), which often occurs by leading 2 months for SOSST and 0 months for Z500 (Liu et al. 2006). It should be noted that the analysis only removes the ENSO variability captured by Niño-3.4 but not by Niño-4 or other ENSO flavors. It is impossible to remove the influence of ENSO completely, at least partially because of the dramatic changes in the face of ENSO (Capotondi et al. 2015).

## 3. Lagged MCA results between SOSST and Z500

Figure 1 shows the SC, SCF, and CORR of the leading lagged MCA mode between SOSST and Z500 anomalies for 1979–2013. The statistically significant results shown in the figure reflect that the dominant ocean–atmosphere interaction feature is the atmospheric forcing for SOSST with a peak at lag(+1), consistent with the results from previous studies for other oceans (e.g., Czaja and Frankignoul 1999, 2002; Sterl and Hazeleger 2003; Huang and Shukla 2005; Liu et al. 2006; Frankignoul and

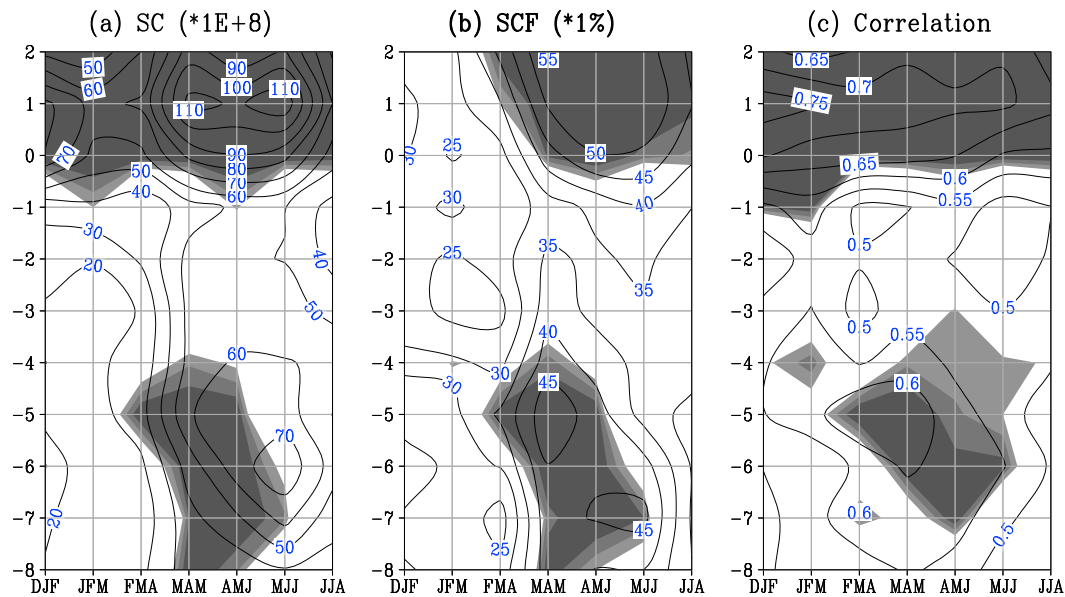


FIG. 1. (a) SC, (b) SCF, and (c) correlation for the first MCA mode between extratropical Z500 (poleward of 20°S) and SST anomalies in the Southern Ocean (20°–70°S) for 1979–2013. Light-to-dark shading respectively indicates those results that exceeding the 85%, 90%, and 95% confidence level in the Monte Carlo test. The abscissa is the Z500 calendar month, while the ordinate is the lagged time of SST, and the negative for SST leading Z500.

(Sennéchal 2007). We also repeat the computations for the OAFlux period of 1979–2008 and obtain results (not shown) consistent with those presented in Fig. 1, indicating that the lagged MCA feature is robust and stable.

Because of our focus on the influence of SOSST on the following atmosphere, we mainly examine the significant results at lags  $< 0$  when SOSST leads MAM Z500. One of the most eye-capturing features in Fig. 1 occurs in austral autumn [MAM–April–June (AMJ)]; see the gray shadings at lags  $< -3$  when the SC, SCF, and CORR are all significant when SOSST leads MAM Z500 by 4–6 months [i.e., from lag(−4) to lag(−6)]. The SCF (CORR) is about 45% (0.6), comparable to the maximum SCF (CORR) that appears when Z500 leads SOSST (Fig. 1), suggesting that the SOSST anomalies have a potential link to the following atmospheric conditions. It is noteworthy that, when SOSST leads Z500, the statistical significance of the results depends clearly on season and lag time, due possibly to the higher signal-to-noise ratio during particular seasons (i.e., MAM–AMJ) and the lag time after removing ENSO signals and linear trends to a certain extent. For example, ENSO is often in its mature stage during boreal winter [December–February (DJF)–January–March (JFM)], and after removing the ENSO signals, even if partially, the residual cross-seasonal MCA values (i.e., SC, SCF, and CORR) between the DJF–JFM SOSST and the MAM Z500 are relatively small compared with many other random trials, leading to the insignificances in the

Monte Carlo test (Fig. 1) when SOSST leads MAM Z500 by 1–3 months i.e., from lag(−1) to lag(−3).

#### a. Cross-seasonal patterns coupled between SOSST and Z500

This section is focused only on the significant coupled modes when Z500 is fixed for MAM, which may infer the potential link between MAM Z500 and preceding SOSST. Figure 2 shows the coupled patterns from lag(−8) to lag(−4) and from lag(−0) to lag(+2) when SC, SCF, and CORR are found at the 5% or 10% significance levels (Fig. 1), except for CORR at lag(−8) and lag(−7). Each coupled pattern preserves a covariant linear relationship between MAM Z500 and SOSST at each lagged season (Figs. 2a–h). For all lags, the MCA-Z500 patterns (Fig. 2, in which Z500 is always fixed for MAM) are similar to the first EOF mode of MAM Z500 (not shown), and the MCA-Z500 time coefficients are all highly correlated to the MAM AAO index ( $r > 0.9$ , exceeding the 99.9% confidence level). Thus hereafter the atmospheric signals in MAM (Figs. 2a–h, the MCA-Z500 patterns) are referred to as the AAO modes, with large opposite Z500 anomalies reaching 20–35 gpm over the SH midlatitudes and high latitudes. It is therefore suggested that the MAM AAO variability is significantly linked to the preceding SOSST anomalies from austral spring to early summer. Similar coupled patterns (not shown) are found at lag(−4) to lag(−7) when Z500 is fixed for AMJ (see Fig. 1).

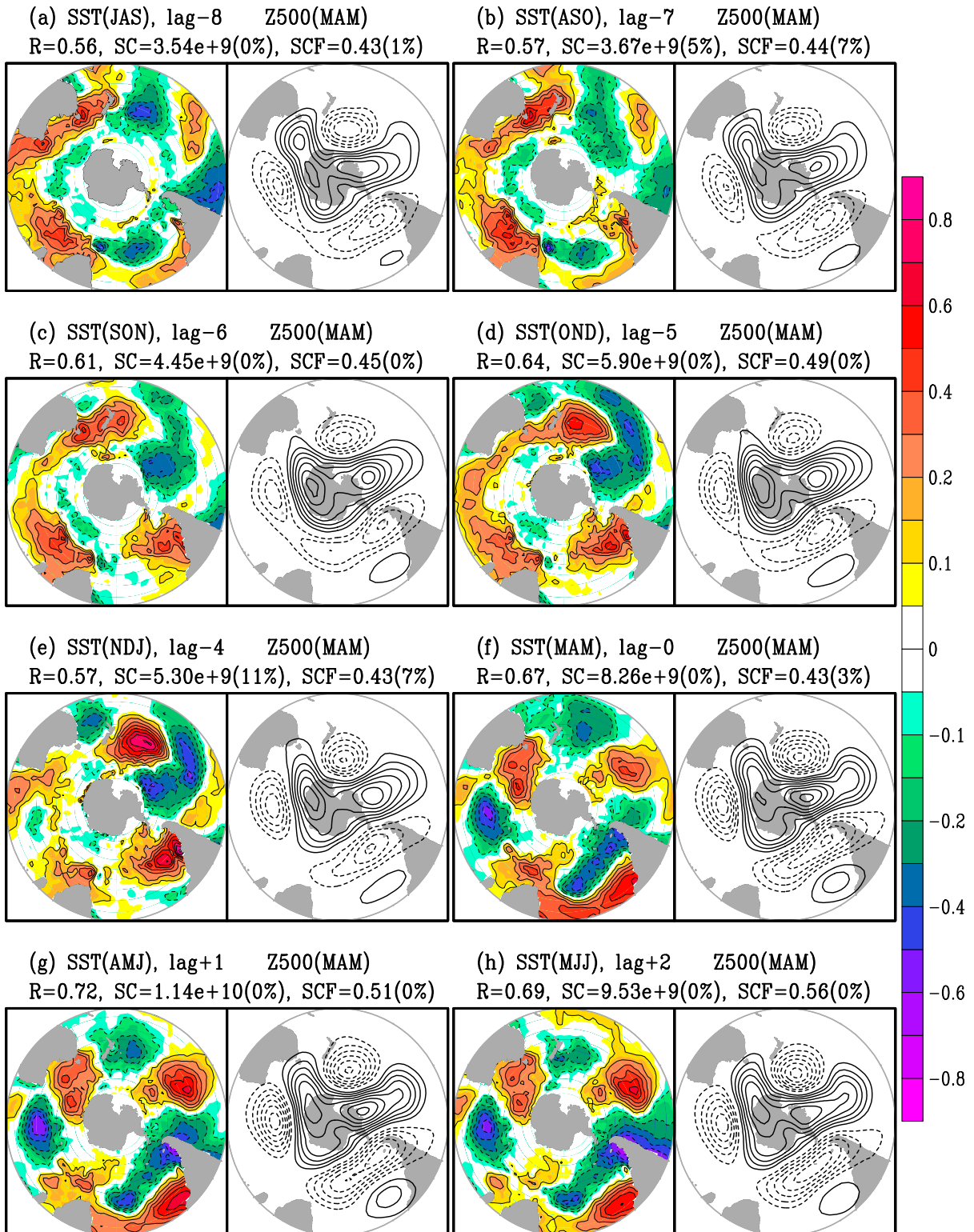


FIG. 2. Maximum covariance regression maps for (top) homogeneous SST and (bottom) heterogeneous Z500 anomalies (Z500 is always fixed for MAM; SST is lagged as indicated). The contour interval is 5 gpm for Z500 and the unit for SST is 0.05 K; the negative contours are dashed; and the zero line is omitted. The time series have been normalized so that the figure shows typical amplitudes. The correlation  $R$ , SC, and SCF are indicated at the estimated significance level of the Monte Carlo test.

TABLE 1. Correlation matrix of MCA-SST/Z500 time series and Niño-3.4 at each lag/season (e.g., lag $-6$  and lag $0$  denote SON and MAM, respectively). Note here the Niño-3.4 is simultaneous to the MCA-SST time series at each lag.

Correlation	Lag( $-8$ )	Lag( $-7$ )	Lag( $-6$ )	Lag( $-5$ )	Lag( $-4$ )	Lag( $-3$ )	Lag( $-2$ )	Lag( $-1$ )	Lag( $0$ )	Lag( $+1$ )	Lag( $+2$ )
MCA-SST	-0.02	-0.02	0.01	0.01	0.03	0.08	-0.01	-0.01	0.04	0.02	0.02
MCA-Z500	-0.12	-0.13	-0.05	0.07	0.14	0.15	-0.12	0.06	0.01	0.04	0.04

In contrast to the results shown in Figs. 2a–e describing the significant SOSST precursory signals of MAM AAO, the dominant relationships depicted in Figs. 2f–h are the effect of atmosphere on the SOSST at lag( $0$ ), lag( $+1$ ), and lag( $+2$ ). The spatial structure (Figs. 2c–e) of the MCA-SST is approximately quadrupole, exhibiting an out-of-phase relationship among the SST anomalies in the Indian Ocean, Pacific, and Atlantic sectors of the Southern Ocean. Furthermore, the adjacent MCA-SST time coefficients are significantly correlated with each other ( $r > 0.6$ , over the 99.9% confidence level of the Student's  $t$  test), indicating that the progression of the SOSST anomalies is well coordinated both spatially and temporally.

Such robust signals may provide useful information for predicting the SH extratropical atmospheric circulation in austral autumn from the perspective of the cross-seasonal relationship established above. Two more points should be emphasized. First, such significant links between the SOSST anomalies and the MAM AAO are not significantly affected by the ENSO signals represented by Niño-3.4 (see Tables 1 and 2) and linear trends, which have been removed to a certain extent before performing the lagged MCA. Second, the atmospheric response in austral autumn not only may reflect the simultaneous or preceding SOSST forcing, but also can indicate that the establishment of the atmospheric response process may take a longer time than that commonly assumed (see Ferreira and Frankignoul 2005; Francis et al. 2009).

#### b. Persistence of SOSST patterns

As shown in Fig. 2, the significant lagged MCA results (say, the SC, SCF, and CORR in Fig. 1) between MAM Z500 and preceding SOSST seem to be related to the gradual evolution of continuous SOSST anomalies. If this is the case, such a signal in the gradual evolution of MCA-SST patterns may also be found implicitly in the SOSST due to the persistence of SOSST anomalies induced by the “oceanic memory” and the thermal inertia

of ocean mixed layer (e.g., Frankignoul and Hasselmann 1977; Ciasto et al. 2011). Regressing the SOSST fields of July–September (JAS), August–October (ASO), September–November (SON), October–December (OND), November–January (NDJ), DJF, JFM, February–April (FMA), MAM, and April–June (AMJ) onto the normalized SON MCA-SST time series at lag( $-6$ ) (Fig. 3), which mirrors the memory modes of SOSST anomalies, yields features similar to those shown in Fig. 2. These memory modes imply that the SOSST anomalies are persistent and partly explain why such cross-seasonal covariability, which presumably takes place between the preceding SOSST anomalies from austral spring to early autumn and the atmospheric circulation in austral autumn, can be captured clearly by the lagged MCA.

#### c. Possible cause of the gradual evolution of MCA-SST anomalies

The persistence of SST anomalies varies with seasons (e.g., Frankignoul 1985), which reflects not only the changes in the thermal inertia of ocean mixed layer (Frankignoul and Hasselmann 1977) but also other feedback processes such as the response of oceanic surface layer to atmospheric forcing (Hasselmann 1976), especially the surface heat flux exchange in the air–sea interface (e.g., Frankignoul et al. 1998; Wen et al. 2005; Frankignoul and Sennéchal 2007). Surface heat flux as an important quantity in ocean–atmosphere interaction plays an important role in regulating climate variations. Specifically, it comprises turbulent heat flux (LQSQ, latent heat flux plus sensible heat flux) and radiative flux. LQSQ is proportional to wind speed and air–sea temperature or humidity difference, while radiative flux is a function of air temperature, humidity, and cloudiness (Peixoto and Oort 1992). Previous studies have shown that the influence of atmospheric internal variability on LQSQ is much stronger than on SST (Houghton 1991; Cayan 1992; Yu et al. 2006). Moreover, both modeling

TABLE 2. As in Table 1, but here the Niño-3.4 leads MCA-SST time series by 2 months and MCA-Z500 time series by 0 month at each lag.

Correlation	Lag( $-8$ )	Lag( $-7$ )	Lag( $-6$ )	Lag( $-5$ )	Lag( $-4$ )	Lag( $-3$ )	Lag( $-2$ )	Lag( $-1$ )	Lag( $0$ )	Lag( $+1$ )	Lag( $+2$ )
MCA-SST	-0.01	0.00	0.01	0.00	0.00	0.04	-0.01	0.01	-0.02	-0.03	-0.02
MCA-Z500	0.00	0.00	0.01	-0.01	0.00	0.00	0.01	-0.01	0.01	0.01	0.01

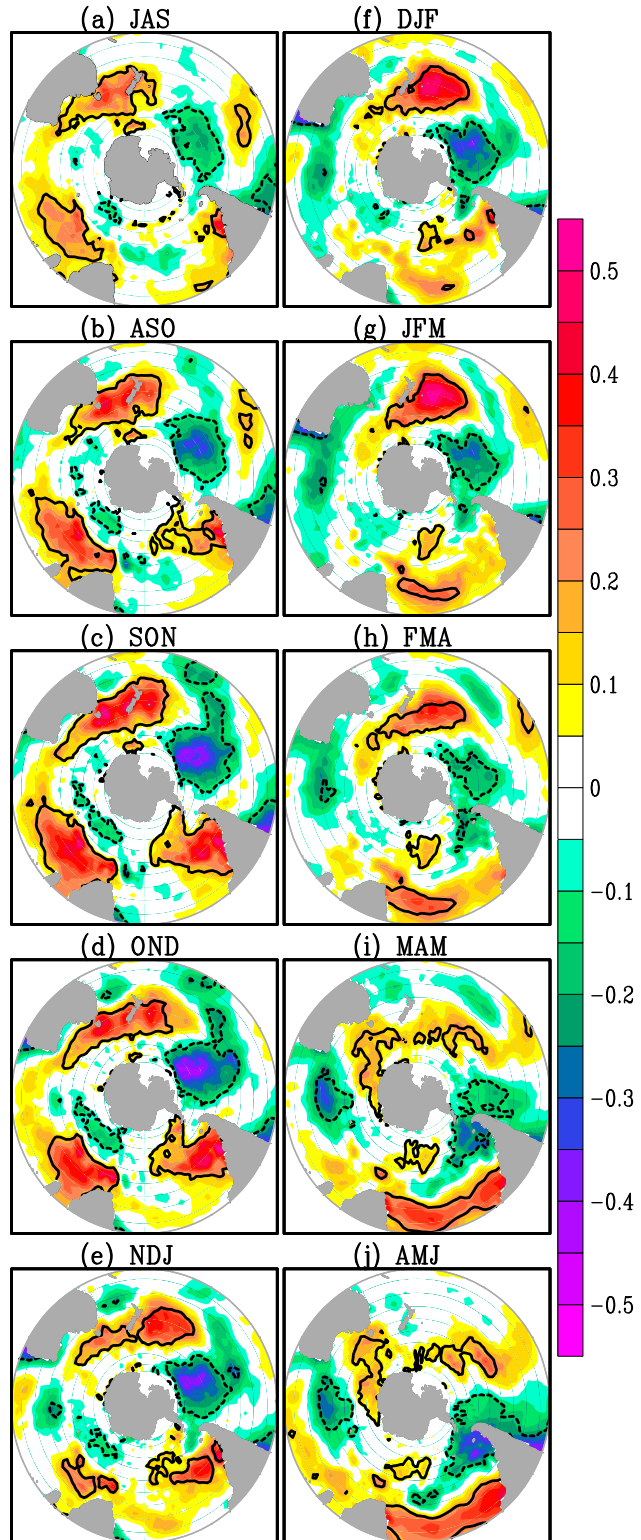


FIG. 3. Regression maps of SST anomalies in (a) JAS, (b) ASO, (c) SON, (d) OND, (e) NDJ, (f) DJF, (g) JFM, (h) FMA, (i) MAM, and (j) AMJ onto the MCA-SST time series at lag(-6). The unit for SST is 0.05 K; the negative contours are dashed; and the zero line is omitted. The thick lines indicate correlation at the estimated 1% significance level.

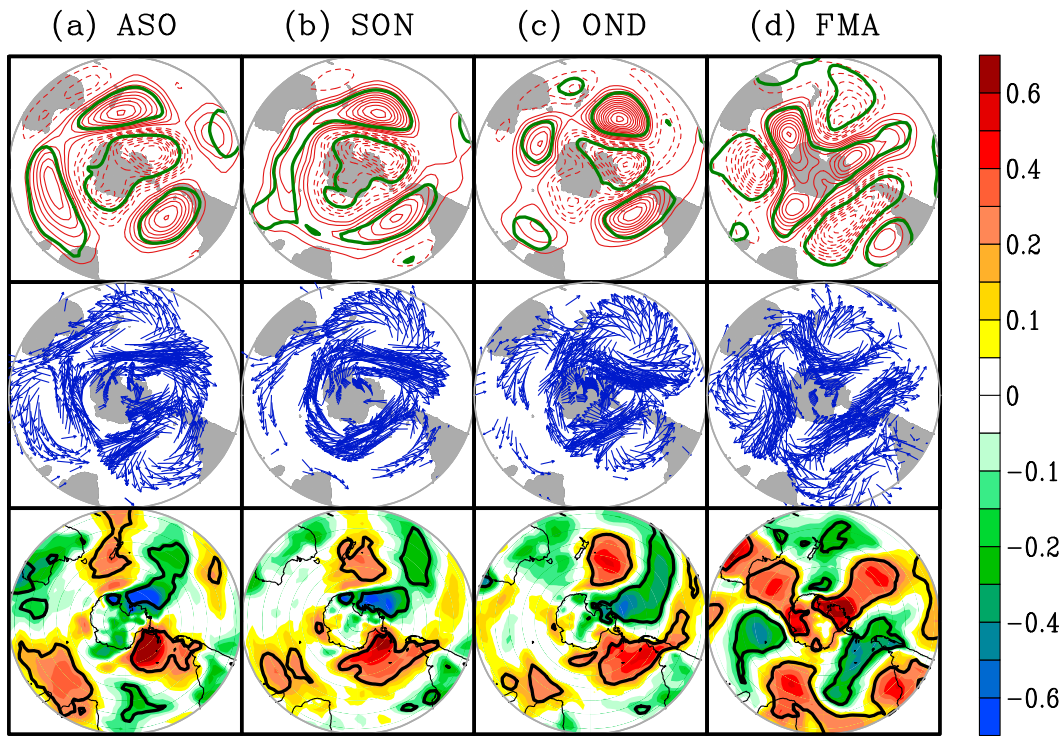


FIG. 4. Regression maps of (top) Z500, (middle) UV925, and (bottom) T925 anomalies in (a) ASO, (b) SON, (c) OND, and (d) FMA onto the normalized MCA-SST time series one month later correspondingly. For example, (a) at (top) is for the regressed map of ASO Z500 onto the SON MCA-SST time series. The contour interval is 2.5 gpm for Z500; the negative contours are dashed; and the zero line is omitted. Only vectors with a significant  $u$  or  $v$  component over the estimated 5% significance level are plotted. The thick lines indicate correlation at the estimated 5% significance level for Z500 and T925, respectively.

and observational studies have suggested that the SOSST anomalies associated with AAO are largely generated via the changes in LQSQ (e.g., Hall and Visbeck 2002; Verdy et al. 2006; Sen Gupta and England 2006; Ciasto and Thompson 2008). Thus, the SOSST patterns may be caused by the intrinsic modes of atmospheric variability that imprint themselves upon the SOSST field, mainly via LQSQ associated with cold or warm advection.

Accordingly, to determine how the MCA-SST evolution is linked to the changes in atmospheric circulation and LQSQ, we plot the patterns of lagged regressions of Z500, winds, T925, SLP, and LQSQ onto the normalized MCA-SST time series one month later (Figs. 4 and 5), because the effect of atmosphere on SOSST is the dominant feature of air-sea interaction that often appears when Z500 leads SOSST by one month (Fig. 1). The Z500-UV925-SLP patterns are first dominated by a positive AAO-like mode (Figs. 4a and 5a) with a strong anomalous low or cyclone over the Antarctic Peninsula and opposite-sign anomalies around it over the Southern Ocean. However, this AAO mode becomes narrower and weaker gradually (Figs. 4a–c). In early austral autumn (FMA–MAM), the AAO features an opposite

phase (Figs. 4d, 5b, and 2) with a robust anomalous anticyclone over the Antarctic Peninsula, suggesting that the change in the phase of the AAO is directly linked to the change in the SOSST pattern (Figs. 2 and 3). The corresponding spatial structures of cold or warm advection (UV925 and T925) in ASO (Fig. 4a) and FMA (Fig. 4d), as well as LQSQ in ASO (Fig. 5a, top) and FMA (Fig. 5b, top), contribute to the generations of SOSST anomalies one month later in SON (Fig. 5a, bottom) and MAM (Fig. 5b, bottom), respectively. The positive LQSQ shown in Figs. 5a and 5b indicates that heat flux is transferred from oceans to the atmosphere, which is accompanied by cold advection (UV925 and T925 in Figs. 4a,d), corresponding to the negative SOSST anomalies one month later (Figs. 5a,b), and vice versa, although with some excursion due possibly to the effects of the Antarctic sea ice (Wu and Zhang 2011) and to a less extent the Ekman transport (e.g., Sen Gupta and England 2007; Ciasto and Thompson 2008).

In other words, the intrinsic mode of atmospheric variability modulates SOSST mainly via LQSQ and thus it acts as a generation forcing on the SOSST later, suggesting that air-sea heat exchange controls the seasonal

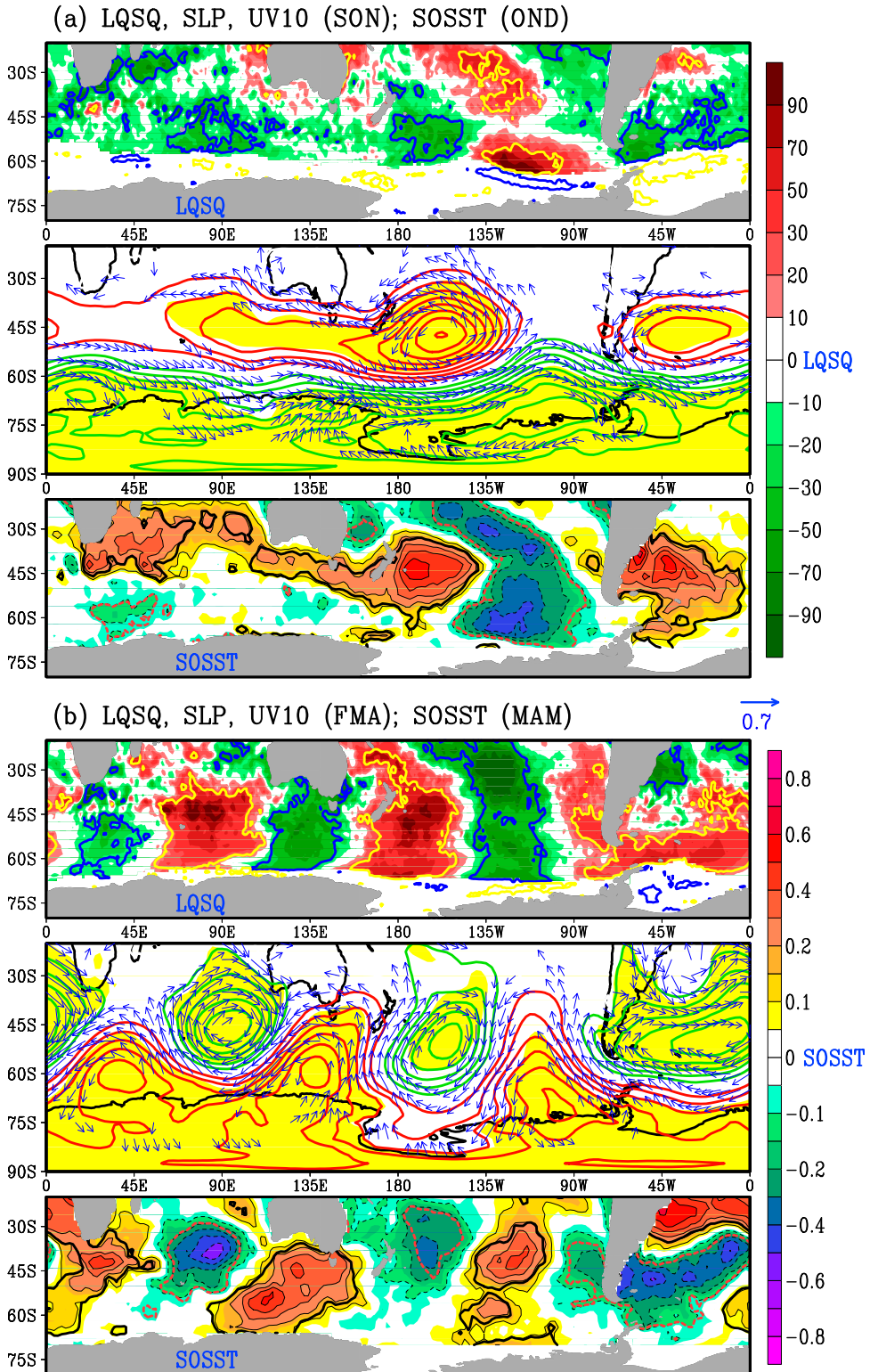


FIG. 5. Regressions (a) of (top) LQSQ and (middle) SLP (contour) anomalies in SON, and (bottom) SST anomalies in OND onto the normalized MCA-SST time series in OND. Also shown is the correlation between the SON surface wind anomalies (middle; arrow) and the OND MCA-SST time series. (b) As in (a), but for LOSQ, SLP, surface wind in FMA and SST in MAM, and the MCA-SST time series in MAM. The contour interval is 0.3 hPa for SLP; and the zero line is omitted. The unit for LQSQ is  $\text{W m}^{-2}$  and the unit for SST is 0.05 K. The thick lines (for LQSQ and SST) and yellow shading (for SLP) indicate correlation at the estimated 5% significance level, respectively. Only vectors with a significant  $u$  or  $v$  component over the 5% significance level are plotted.

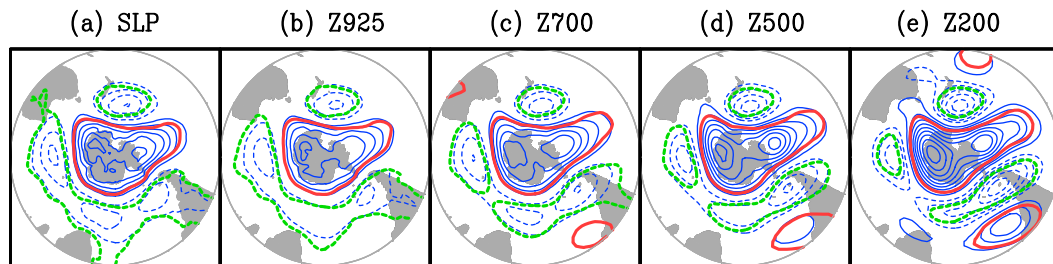


FIG. 6. Regressions of (a) SLP, (b) Z925, (c) Z700, (d) Z500, and (e) Z200 anomalies (after removing ENSO signals and long-term trends) in MAM onto the normalized MCA-SST time series at lag(−6). The contour interval is 0.5 hPa for SLP and 5 gpm for Z925, Z700, Z500, and Z200; the negative contours are dashed; and the zero line is omitted. The thick lines indicate correlation at the estimated 5% significance level.

variations of SOSST and in turn the seasonal to interannual climate variability (e.g., Houghton 1991; Cayan 1992; Yu et al. 2006). Such a phenomenon implies that SOSST anomalies are at least partly generated by the LQSQ forcing associated with atmospheric cold or warm advection.

#### 4. Verifications of cross-seasonal MCA results with regression analyses

To enable a more comprehensive examination of the atmospheric circulation anomalies that follow persistent SOSST anomalies, we further conduct a regression reanalysis (Fig. 6) of the MAM anomaly fields of SLP, Z925, Z700, Z500, and Z200, after removing ENSO signals and linear trends, onto the normalized MCA-SST time series at lag(−6) when SC, SCF, and CORR are all significant. The main finding from the regression analysis is that the negative AAO-like signals are largely quasi-barotropic throughout the troposphere, consistent with the barotropic atmospheric response to reduced Antarctic SIC as shown by Wu and Zhang (2011).

Furthermore, we attempt to detect which part of the SON SOSST anomalies at lag(−6), chosen because the SC, SCF, and CORR are all significant and with lead time up to two seasons, possesses a strongest link with the following autumn AAO. Based on the area-averaged SST anomalies in four main centers of the MCA-SST pattern at lag(−6), namely, box 1 ( $25^{\circ}$ – $45^{\circ}$ S,  $25^{\circ}$ – $75^{\circ}$ E), box 2 ( $35^{\circ}$ – $55^{\circ}$ S,  $140^{\circ}$ – $195^{\circ}$ E), box 3 ( $45^{\circ}$ – $65^{\circ}$ S,  $145^{\circ}$ – $95^{\circ}$ W), and box 4 ( $32^{\circ}$ – $52^{\circ}$ S,  $70^{\circ}$ – $30^{\circ}$ W), we construct four indices, plus a fifth index referred to as “box1–4” computed as (box 1 + box 2 – box 3 + box 4)/4. Then, by projecting the MAM Z500 anomalies onto the five indices, we obtain the Z500 anomaly patterns (Fig. 7). It turns out that these patterns resemble the pattern obtained from the lagged MCA in Fig. 2c, with the most robust link to MAM AAO when all four centers are considered together (Fig. 7e), suggesting that all centers of action seem to be

related to the AAO collaboratively. Therefore, a new and more straightforward way to foresee SH climate anomalies can be expected from the lagged relationships established. Note that these box-based calculations are independent of the MCA, except for the choice of box locations and lagged seasons, indicating that the above lagged MCA results are robust and reliable.

#### 5. Summary and discussion

Using the lagged MCA, we have investigated the cross-seasonal relationship between SOSST and Z500 in the Southern Hemisphere based on the climate variability observed in the recent decades. It is demonstrated that large-scale atmospheric circulation plays a dominant role in forcing SOSST with a peak at lag(+1) but the austral autumn AAO variability is associated with the preceding austral spring-to-summer SST anomalies of the Southern Ocean. Our results are in agreement with those from the previous modeling studies by Watterson (2001), Marshall and Connolley (2006), and Sen Gupta and England (2006, 2007), who found that the atmosphere was sensitive to Southern Ocean SST anomalies. The link between MAM AAO and preceding SOSST anomalies seems to stem from the large persistence and the gradual evolution of SOSST anomalies. Nevertheless, such persistence and evolution could be explained by dynamical and thermodynamic processes in which the gradual evolution of SOSST anomalies is due mainly to the complex air-sea interaction (e.g., surface heat flux exchange and cold/warm advection). The significant link between preceding SOSST and SH atmospheric circulation may have an implication for skillful prediction of MAM AAO from the perspective of SOSST anomalies with lead time up to 6–7 months.

It is important to note that the significant lagged MCA results are only detected in certain calendar months after removing ENSO signals due possibly to the high signal-to-noise ratio on seasonal to interannual time

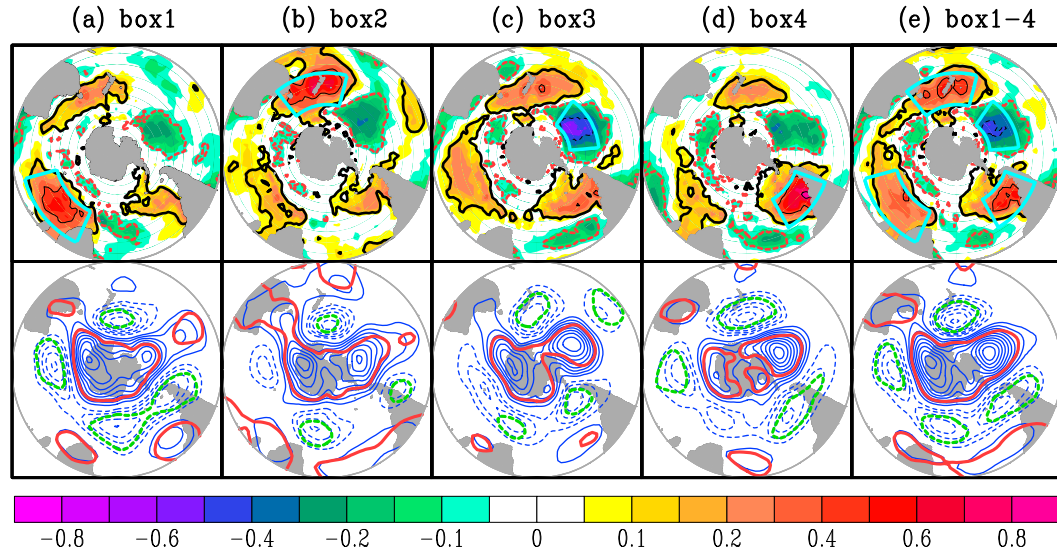


FIG. 7. Regression maps of the SON SOSST and the MAM Z500 anomaly fields against the five box-based SST indices in SON (after removing ENSO signals and long-term trends). These indices are separately defined as the area-averaged SST anomalies in the sky-blue (a) box 1 ( $25^{\circ}$ – $45^{\circ}$ S,  $25^{\circ}$ – $75^{\circ}$ E), (b) box 2 ( $35^{\circ}$ – $55^{\circ}$ S,  $140^{\circ}$ – $195^{\circ}$ E), (c) box 3 ( $45^{\circ}$ – $65^{\circ}$ S,  $145^{\circ}$ – $95^{\circ}$ W) and (d) box 4 ( $32^{\circ}$ – $52^{\circ}$ S,  $70^{\circ}$ – $30^{\circ}$ W); (e) “box1–4” represents (box 1 + box 2 – box 3 + box 4)/4. The contour interval is 2.5 gpm for Z500 and the unit for SST is 0.05 K; the negative contours are dashed; and the zero line is omitted. The thick lines indicate correlation exceeding the 0.1 significance level for Z500 and SST.

scales, indicating that there exists a remarkable sensitivity in terms of lagged time and seasonality. Our results support previous GCM sensitivity studies in that the atmospheric response to midlatitude SST anomalies strongly depends on the background circulation state, which can change substantially from one month to the next (Peng et al. 1997; Peng and Whitaker 1999; Peng and Robinson 2001). This feature has been seen for the North Atlantic (Czaja and Frankignoul 1999, 2002) and the North Pacific (Frankignoul and Sennéchael 2007; Liu et al. 2006).

It should be cautioned that although we have focused on detecting the impact of SOSST anomalies on SH large-scale atmospheric circulation and the regression analysis based on SOSST anomaly centers confirms our findings, it is also possible that the relationship between the austral autumn AAO and early-season SOSST anomalies is affected by a third external forcing (e.g., Antarctic sea ice, other ENSO flavors, the India Ocean dipole, North Atlantic SST, etc.), even though the influences of long-term trend and Niño-3.4 signals have been removed to a certain extent. Finally, it should be pointed out that the results obtained in this study are based on analyses of the climate in the period of 1979–2013 or 1979–2008 when satellite observations are available. It is also important if the relationships among SOSST, surface turbulent heat flux exchange, cold/warm advection, and atmospheric circulation can be further confirmed by longer data records.

**Acknowledgments.** The authors thank the three anonymous reviewers who have provided helpful comments and suggestions for improving the overall quality of the paper, and Prof. Yi Deng of the Georgia Institute of Technology and Prof. Mingfang Ting of Columbia University for their helpful discussions. The study was supported by the National Key Scientific Research Plan of China (Grants 2012CB956002 and 2014CB953900), the National Natural Science Foundation of China (Grant 41375081), the China Special Fund for Meteorological Research in the Public Interest (Grant 201206038), the LASW State Key Laboratory Special Fund (2013LASW-A05), and the Jiangsu Collaborative Innovation Center for Climate Change. Calculations for this study were supported by the China National Supercomputer Center in Guangzhou.

## REFERENCES

- Cai, W., and P. G. Baines, 2001: Forcing of the Antarctic circum-polar wave by El Niño–Southern Oscillation teleconnections. *J. Geophys. Res.*, **106**, 9019–9038, doi:[10.1029/2000JC000590](https://doi.org/10.1029/2000JC000590).
- Capotondi, A., and Coauthors, 2015: Understanding ENSO diversity. *Bull. Amer. Meteor. Soc.*, **96**, 921–938, doi:[10.1175/BAMS-D-13-00117.1](https://doi.org/10.1175/BAMS-D-13-00117.1).
- Cayan, D. R., 1992: Latent and sensible heat flux anomalies over the northern oceans: Driving the sea surface temperature. *J. Phys. Oceanogr.*, **22**, 859–881, doi:[10.1175/1520-0485\(1992\)022<0859:LASHFA>2.0.CO;2](https://doi.org/10.1175/1520-0485(1992)022<0859:LASHFA>2.0.CO;2).
- Ciazzo, L. M., and D. W. J. Thompson, 2008: Observations of large-scale ocean–atmosphere interaction in the Southern

- Hemisphere. *J. Climate*, **21**, 1244–1259, doi:[10.1175/2007JCLI1809.1](https://doi.org/10.1175/2007JCLI1809.1).
- , M. A. Alexander, C. Deser, and M. H. England, 2011: Air-sea feedback in the North Atlantic and surface boundary conditions for ocean models. *J. Climate*, **24**, 2500–2515, doi:[10.1175/2010JCLI3535.1](https://doi.org/10.1175/2010JCLI3535.1).
- Codron, F., 2005: Relation between annular modes and the mean state: Southern Hemisphere summer. *J. Climate*, **18**, 320–330, doi:[10.1175/JCLI-3255.1](https://doi.org/10.1175/JCLI-3255.1).
- , 2007: Relations between annular modes and the mean state: Southern Hemisphere winter. *J. Atmos. Sci.*, **64**, 3328–3339, doi:[10.1175/JAS4012.1](https://doi.org/10.1175/JAS4012.1).
- Czaja, A., and C. Frankignoul, 1999: Influence of the North Atlantic SST on the atmospheric circulation. *Geophys. Res. Lett.*, **26**, 2969–2972, doi:[10.1029/1999GL900613](https://doi.org/10.1029/1999GL900613).
- , and —, 2002: Observed impact of Atlantic SST anomalies on the North Atlantic Oscillation. *J. Climate*, **15**, 606–623, doi:[10.1175/1520-0442\(2002\)015<0606:OIOASA>2.0.CO;2](https://doi.org/10.1175/1520-0442(2002)015<0606:OIOASA>2.0.CO;2).
- Dee, D. P., and Coauthors, 2011: The ERA-Interim reanalysis: Configuration and performance of the data assimilation system. *Quart. J. Roy. Meteor. Soc.*, **137**, 553–597, doi:[10.1002/qj.828](https://doi.org/10.1002/qj.828).
- Ding, Q., E. J. Steig, D. S. Battisti, and M. Küttel, 2011: Winter warming in West Antarctica caused by central tropical Pacific warming. *Nat. Geosci.*, **4**, 398–403, doi:[10.1038/ngeo1129](https://doi.org/10.1038/ngeo1129).
- , —, —, and J. M. Wallace, 2012: Influence of the tropics on the southern annular mode. *J. Climate*, **25**, 6330–6348, doi:[10.1175/JCLI-D-11-00523.1](https://doi.org/10.1175/JCLI-D-11-00523.1).
- Fan, K., and H. Wang, 2004: Antarctic Oscillation and the dust weather frequency in North China. *Geophys. Res. Lett.*, **31**, L10201, doi:[10.1029/2004GL019465](https://doi.org/10.1029/2004GL019465).
- , and —, 2006: Interannual variability of Antarctic Oscillation and its influence on East Asian climate during boreal winter and spring. *Sci. China*, **49D**, 554–560, doi:[10.1007/s11430-006-0554-7](https://doi.org/10.1007/s11430-006-0554-7).
- Ferreira, D., and C. Frankignoul, 2005: The transient atmospheric response to midlatitude SST anomalies. *J. Climate*, **18**, 1049–1067, doi:[10.1175/JCLI-3313.1](https://doi.org/10.1175/JCLI-3313.1).
- Francis, J. A., W. Chan, D. J. Leathers, J. R. Miller, and D. E. Veron, 2009: Winter Northern Hemisphere weather patterns remember summer Arctic sea-ice extent. *Geophys. Res. Lett.*, **36**, L07503, doi:[10.1029/2009GL037274](https://doi.org/10.1029/2009GL037274).
- Frankignoul, C., 1985: Sea surface temperature anomalies, planetary waves, and air-sea feedback in the middle latitudes. *Rev. Geophys.*, **23**, 357–390, doi:[10.1029/RG023i004p00357](https://doi.org/10.1029/RG023i004p00357).
- , and K. Hasselmann, 1977: Stochastic climate models. Part II: Application to sea-surface temperature variability and thermocline variability. *Tellus*, **29A**, 289–305, doi:[10.1111/j.2153-3490.1977.tb00740.x](https://doi.org/10.1111/j.2153-3490.1977.tb00740.x).
- , and N. Sennéchal, 2007: Observed influence of North Pacific SST anomalies on the atmospheric circulation. *J. Climate*, **20**, 592–606, doi:[10.1175/JCLI4021.1](https://doi.org/10.1175/JCLI4021.1).
- , A. Czaja, and B. L'Heveder, 1998: Air-sea feedback in the North Atlantic and surface boundary conditions for ocean models. *J. Climate*, **11**, 2310–2324, doi:[10.1175/1520-0442\(1998\)011<2310:ASFITN>2.0.CO;2](https://doi.org/10.1175/1520-0442(1998)011<2310:ASFITN>2.0.CO;2).
- , N. Chouaib, and Z. Liu, 2011: Estimating the observed atmospheric response to SST anomalies: Maximum covariance analysis, generalized equilibrium feedback assessment, and maximum response estimation. *J. Climate*, **24**, 2523–2539, doi:[10.1175/2010JCLI3696.1](https://doi.org/10.1175/2010JCLI3696.1).
- , N. Sennéchal, and P. Cauchy, 2014: Observed atmospheric response to cold season sea ice variability in the Arctic. *J. Climate*, **27**, 1243–1254, doi:[10.1175/JCLI-D-13-00189.1](https://doi.org/10.1175/JCLI-D-13-00189.1).
- Gillet, N. P., and D. W. J. Thompson, 2003: Simulation of recent Southern Hemisphere climate change. *Science*, **302**, 273–275, doi:[10.1126/science.1087440](https://doi.org/10.1126/science.1087440).
- , T. D. Kell, and P. D. Jones, 2006: Regional climate impacts of the southern annular mode. *Geophys. Res. Lett.*, **33**, L23704, doi:[10.1029/2006GL027721](https://doi.org/10.1029/2006GL027721).
- Gong, D., and S. Wang, 1999: Definition of Antarctic Oscillation index. *Geophys. Res. Lett.*, **26**, 459–462, doi:[10.1029/1999GL900003](https://doi.org/10.1029/1999GL900003).
- Hall, A., and M. Visbeck, 2002: Synchronous variability in the Southern Hemisphere atmosphere, sea ice, and ocean resulting from the annular mode. *J. Climate*, **15**, 3043–3057, doi:[10.1175/1520-0442\(2002\)015<3043:SVITSH>2.0.CO;2](https://doi.org/10.1175/1520-0442(2002)015<3043:SVITSH>2.0.CO;2).
- Hartmann, D. L., and F. Lo, 1998: Wave-driven zonal flow vacillation in the Southern Hemisphere. *J. Atmos. Sci.*, **55**, 1303–1315, doi:[10.1175/1520-0469\(1998\)055<1303:WDZFVI>2.0.CO;2](https://doi.org/10.1175/1520-0469(1998)055<1303:WDZFVI>2.0.CO;2).
- Hasselmann, K., 1976: Stochastic climate models. Part I: Theory. *Tellus*, **28A**, 473–485, doi:[10.1111/j.2153-3490.1976.tb00696.x](https://doi.org/10.1111/j.2153-3490.1976.tb00696.x).
- Houghton, R. W., 1991: The relationship of sea surface temperature to thermocline depth at annual and interannual time scales in the tropical Atlantic Ocean. *J. Geophys. Res.*, **96**, 15 173–15 185, doi:[10.1029/91JC01442](https://doi.org/10.1029/91JC01442).
- Huang, B., and J. Shukla, 2005: Ocean–atmosphere interactions in the tropical and subtropical Atlantic Ocean. *J. Climate*, **18**, 1652–1672, doi:[10.1175/JCLI3368.1](https://doi.org/10.1175/JCLI3368.1).
- Karoly, D. J., 1989: Southern Hemisphere circulation features associated with El Niño–Southern Oscillation events. *J. Climate*, **2**, 1239–1252, doi:[10.1175/1520-0442\(1989\)002<1239:SHCFAW>2.0.CO;2](https://doi.org/10.1175/1520-0442(1989)002<1239:SHCFAW>2.0.CO;2).
- Kidson, J. W., 1988: Interannual variations in the Southern Hemisphere circulation. *J. Climate*, **1**, 1177–1198, doi:[10.1175/1520-0442\(1988\)001<1177:IVITSH>2.0.CO;2](https://doi.org/10.1175/1520-0442(1988)001<1177:IVITSH>2.0.CO;2).
- Kistler, R., and Coauthors, 2001: The NCEP–NCAR 50-Year Reanalysis: Monthly means CD-ROM and documentation. *Bull. Amer. Meteor. Soc.*, **82**, 247–267, doi:[10.1175/1520-0477\(2001\)082<0247:TNNYRM>2.3.CO;2](https://doi.org/10.1175/1520-0477(2001)082<0247:TNNYRM>2.3.CO;2).
- Kushnir, Y., W. Robinson, I. Bladé, N. Hall, S. Peng, and R. Sutton, 2002: Atmospheric GCM response to extratropical SST anomalies: Synthesis and evaluation. *J. Climate*, **15**, 2233–2256, doi:[10.1175/1520-0442\(2002\)015<2233:AGRTE>2.0.CO;2](https://doi.org/10.1175/1520-0442(2002)015<2233:AGRTE>2.0.CO;2).
- Lachlan-Cope, T., 2005: Role of sea ice in forcing the winter climate of Antarctica in a global climate model. *J. Geophys. Res.*, **110**, D03110, doi:[10.1029/2004JD004935](https://doi.org/10.1029/2004JD004935).
- Lim, E.-P., H. H. Hendon, and H. Rashid, 2013: Seasonal predictability of the southern annular mode due to its association with ENSO. *J. Climate*, **26**, 8037–8054, doi:[10.1175/JCLI-D-13-00006.1](https://doi.org/10.1175/JCLI-D-13-00006.1).
- Limpasuvan, V., and D. L. Hartmann, 2000: Wave-maintained annular modes of climate variability. *J. Climate*, **13**, 4414–4429, doi:[10.1175/1520-0442\(2000\)013<4414:WMAMOC>2.0.CO;2](https://doi.org/10.1175/1520-0442(2000)013<4414:WMAMOC>2.0.CO;2).
- Liu, Q., N. Wen, and Z. Liu, 2006: An observational study of the impact of the North Pacific SST on the atmosphere. *Geophys. Res. Lett.*, **33**, L18611, doi:[10.1029/2006GL026082](https://doi.org/10.1029/2006GL026082).
- Lorenz, D. J., and D. L. Hartmann, 2001: Eddy-zonal flow feedback in the Southern Hemisphere. *J. Atmos. Sci.*, **58**, 3312–3327, doi:[10.1175/1520-0469\(2001\)058<3312:EZZFF>2.0.CO;2](https://doi.org/10.1175/1520-0469(2001)058<3312:EZZFF>2.0.CO;2).
- Lovenduski, N. S., and N. Gruber, 2005: Impact of the southern annular mode on Southern Ocean circulation and biology. *Geophys. Res. Lett.*, **32**, L11603, doi:[10.1029/2005GL022727](https://doi.org/10.1029/2005GL022727).
- Mantua, N. J., S. R. Hare, Y. Zhang, J. M. Wallace, and R. C. Francis, 1997: A Pacific interdecadal climate oscillation with impacts on salmon production. *Bull. Amer. Meteor. Soc.*, **78**, 1069–1079, doi:[10.1175/1520-0477\(1997\)078<1069:APICOW>2.0.CO;2](https://doi.org/10.1175/1520-0477(1997)078<1069:APICOW>2.0.CO;2).

- Marshall, G. J., and W. M. Connolley, 2006: Effect of changing Southern Hemisphere winter sea surface temperatures on southern annular mode strength. *Geophys. Res. Lett.*, **33**, L17717, doi:[10.1029/2006GL026627](https://doi.org/10.1029/2006GL026627).
- , P. A. Stott, J. Turner, W. M. Connolley, J. C. King, and T. A. Lachlan-Cope, 2004: Causes of exceptional atmospheric circulation changes in the Southern Hemisphere. *Geophys. Res. Lett.*, **31**, L14205, doi:[10.1029/2004GL019952](https://doi.org/10.1029/2004GL019952).
- Miller, R. L., G. A. Schmidt, and D. T. Shindell, 2006: Forced annular variations in the 20th century Intergovernmental Panel on Climate Change Fourth Assessment Report models. *J. Geophys. Res.*, **111**, D18101, doi:[10.1029/2005JD006323](https://doi.org/10.1029/2005JD006323).
- Nakamura, H., G. Lin, and T. Yamagata, 1997: Decadal climate variability in the North Pacific during the recent decades. *Bull. Amer. Meteor. Soc.*, **78**, 2215–2225, doi:[10.1175/1520-0477\(1997\)078<2215:DCVITN>2.0.CO;2](https://doi.org/10.1175/1520-0477(1997)078<2215:DCVITN>2.0.CO;2).
- Nan, S., and J. Li, 2003: The relationship between the summer precipitation in the Yangtze River valley and the boreal spring Southern Hemisphere annular mode. *Geophys. Res. Lett.*, **30**, 2266, doi:[10.1029/2003GL018381](https://doi.org/10.1029/2003GL018381).
- , —, X. Yuan, and P. Zhao, 2009: Boreal spring Southern Hemisphere annular mode, Indian Ocean sea surface temperature, and East Asian summer monsoon. *J. Geophys. Res.*, **114**, D02103, doi:[10.1029/2008JD010045](https://doi.org/10.1029/2008JD010045).
- North, G. R., F. J. Moeng, T. L. Bell, and R. F. Cahalan, 1982a: The latitude dependence of the variance of zonally averaged quantities. *Mon. Wea. Rev.*, **110**, 319–326, doi:[10.1175/1520-0493\(1982\)110<0319:TLDOTV>2.0.CO;2](https://doi.org/10.1175/1520-0493(1982)110<0319:TLDOTV>2.0.CO;2).
- , T. L. Bell, R. F. Cahalan, and F. J. Moeng, 1982b: Sampling errors in the estimation of empirical orthogonal functions. *Mon. Wea. Rev.*, **110**, 699–706, doi:[10.1175/1520-0493\(1982\)110<0699:SEITEO>2.0.CO;2](https://doi.org/10.1175/1520-0493(1982)110<0699:SEITEO>2.0.CO;2).
- Peixoto, J. P., and A. H. Oort, 1992: *Physics of Climate*. American Institute of Physics, 520 pp.
- Peng, S., and J. S. Whitaker, 1999: Mechanisms determining the atmospheric response to midlatitude SST anomalies. *J. Climate*, **12**, 1393–1408, doi:[10.1175/1520-0442\(1999\)012<1393:MDTART>2.0.CO;2](https://doi.org/10.1175/1520-0442(1999)012<1393:MDTART>2.0.CO;2).
- , and W. A. Robinson, 2001: Relationships between atmospheric internal variability and the response to an extratropical SST anomaly. *J. Climate*, **14**, 2943–2959, doi:[10.1175/1520-0442\(2001\)014<2943:RBAIVA>2.0.CO;2](https://doi.org/10.1175/1520-0442(2001)014<2943:RBAIVA>2.0.CO;2).
- , —, and M. P. Hoerling, 1997: The modeled atmospheric response to midlatitude SST anomalies and its dependence on background circulation states. *J. Climate*, **10**, 971–987, doi:[10.1175/1520-0442\(1997\)010<0971:TMARTM>2.0.CO;2](https://doi.org/10.1175/1520-0442(1997)010<0971:TMARTM>2.0.CO;2).
- Raphael, M. N., 2003: Impact of observed sea-ice concentration on the Southern Hemisphere extratropical atmospheric circulation in summer. *J. Geophys. Res.*, **108**, 4687, doi:[10.1029/2002JD003308](https://doi.org/10.1029/2002JD003308).
- , and M. M. Holland, 2006: Twentieth century simulation of the Southern Hemisphere climate in coupled models. Part 1: Large-scale circulation variability. *Climate Dyn.*, **26**, 217–228, doi:[10.1007/s00382-005-0082-8](https://doi.org/10.1007/s00382-005-0082-8).
- Rayner, N. A., D. E. Parker, E. B. Horton, C. K. Folland, L. V. Alexander, D. P. Rowell, E. C. Kent, and A. Kaplan, 2003: Global analyses of sea surface temperature, sea ice, and night marine air temperature since the late nineteenth century. *J. Geophys. Res.*, **108**, 4407, doi:[10.1029/2002JD002670](https://doi.org/10.1029/2002JD002670).
- Renwick, J. A., 2002: Southern Hemisphere circulation and relations with sea ice and sea surface temperature. *J. Climate*, **15**, 3058–3068, doi:[10.1175/1520-0442\(2002\)015<3058:SHCARW>2.0.CO;2](https://doi.org/10.1175/1520-0442(2002)015<3058:SHCARW>2.0.CO;2).
- Sen Gupta, A., and M. H. England, 2006: Coupled ocean-atmosphere-ice response to variations in the southern annular mode. *J. Climate*, **19**, 4457–4486, doi:[10.1175/JCLI3843.1](https://doi.org/10.1175/JCLI3843.1).
- , and —, 2007: Coupled ocean-atmosphere feedback in the southern annular mode. *J. Climate*, **20**, 3677–3692, doi:[10.1175/JCLI4200.1](https://doi.org/10.1175/JCLI4200.1).
- Shen, S. H., and K.-M. Lau, 1995: Biennial oscillation associated with the East Asian summer monsoon and tropical sea surface temperature. *J. Meteor. Soc. Japan*, **73**, 105–124.
- Smith, T. M., R. W. Reynolds, T. C. Peterson, and J. Lawrimore, 2008: Improvements to NOAA's historical merged land-ocean surface temperature analysis (1880–2006). *J. Climate*, **21**, 2283–2296, doi:[10.1175/2007JCLI2100.1](https://doi.org/10.1175/2007JCLI2100.1).
- Sterl, A., and W. Hazleger, 2003: Coupled variability and air-sea interaction in the South Atlantic Ocean. *Climate Dyn.*, **21**, 559–571, doi:[10.1007/s00382-003-0348-y](https://doi.org/10.1007/s00382-003-0348-y).
- Sun, J., 2010: Possible impact of the boreal spring Antarctic Oscillation on the North American summer monsoon. *Atmos. Oceanic Sci. Lett.*, **3**, 232–236, doi:[10.1080/16742834.2010.11446870](https://doi.org/10.1080/16742834.2010.11446870).
- , H. Wang, and W. Yuan, 2010: Linkage of the boreal spring Antarctic Oscillation to the West African summer monsoon. *J. Meteor. Soc. Japan*, **88**, 15–28.
- Thompson, D. W. J., and J. M. Wallace, 2000: Annular modes in the extratropical circulation. Part I: Month-to-month variability. *J. Climate*, **13**, 1000–1016, doi:[10.1175/1520-0442\(2000\)013<1000:AMITEC>2.0.CO;2](https://doi.org/10.1175/1520-0442(2000)013<1000:AMITEC>2.0.CO;2).
- , and S. Solomon, 2002: Interpretation of recent Southern Hemisphere climate change. *Science*, **296**, 895–899, doi:[10.1126/science.1069270](https://doi.org/10.1126/science.1069270).
- Trenberth, K. E., and J. W. Hurrell, 1994: Decadal atmosphere-ocean variations in the Pacific. *Climate Dyn.*, **9**, 303–319, doi:[10.1007/BF00204745](https://doi.org/10.1007/BF00204745).
- Verdy, A., J. Marshall, and A. Czaja, 2006: Sea surface temperature variability along the path of the Antarctic Circumpolar Current. *J. Phys. Oceanogr.*, **36**, 1317–1331, doi:[10.1175/JPO2913.1](https://doi.org/10.1175/JPO2913.1).
- Wang, G., and W. Cai, 2013: Climate-change impact on the 20th-century relationship between the southern annular mode and global mean temperature. *Sci. Rep.*, **3**, 2039, doi:[10.1038/srep02039](https://doi.org/10.1038/srep02039).
- Wang, L., W. Chen, and R. Huang, 2007: Changes in the variability of North Pacific Oscillation around 1975/1976 and its relationship with East Asian winter climate. *J. Geophys. Res.*, **112**, D11110, doi:[10.1029/2006JD008054](https://doi.org/10.1029/2006JD008054).
- , —, and —, 2008: Interdecadal modulation of PDO on the impact of ENSO on the East Asian winter monsoon. *Geophys. Res. Lett.*, **35**, L20702, doi:[10.1029/2008GL035287](https://doi.org/10.1029/2008GL035287).
- , —, W. Zhou, J. C. L. Chan, D. Barriopedro, and R. H. Huang, 2010: Effect of the climate shift around mid-1970s on the relationship between wintertime Ural blocking circulation and East Asian climate. *Int. J. Climatol.*, **30**, 153–158, doi:[10.1002/joc.1876](https://doi.org/10.1002/joc.1876).
- Wang, Z., X. Zhang, Z. Guan, B. Sun, X. Yang, and C. Liu, 2015: An atmospheric origin of the multi-decadal bipolar seesaw. *Sci. Rep.*, **5**, 8909, doi:[10.1038/srep08909](https://doi.org/10.1038/srep08909).
- Watterson, I., 2001: Zonal wind vacillation and its interaction with the ocean: Implications for interannual variability and predictability. *J. Geophys. Res.*, **106**, 23 965–23 975, doi:[10.1029/2000JD000221](https://doi.org/10.1029/2000JD000221).
- Wen, N., Z. Liu, Q. Liu, and C. Frankignoul, 2005: Observations of SST, heat flux and North Atlantic Ocean-atmosphere interaction. *Geophys. Res. Lett.*, **32**, L24619, doi:[10.1029/2005GL024871](https://doi.org/10.1029/2005GL024871).

- White, W. B., R. J. Allan, and R. C. Stone, 2002: Positive feedbacks between the Antarctic circumpolar wave and the global El Niño–Southern Oscillation wave. *J. Geophys. Res.*, **107**, 3165, doi:[10.1029/2000JC000581](https://doi.org/10.1029/2000JC000581).
- Wu, Q., 2008: Observed impact of subtropical–midlatitude South Atlantic SST anomalies on the atmospheric circulation. *Geophys. Res. Lett.*, **35**, L22803, doi:[10.1029/2008GL035488](https://doi.org/10.1029/2008GL035488).
- , 2010: Forcing of tropical SST anomalies by wintertime AO-like variability. *J. Climate*, **23**, 2465–2472, doi:[10.1175/2009JCLI2749.1](https://doi.org/10.1175/2009JCLI2749.1).
- , and X. Zhang, 2010: Observed forcing-feedback processes between Northern Hemisphere atmospheric circulation and Arctic sea ice coverage. *J. Geophys. Res.*, **115**, D14119, doi:[10.1029/2009JD013574](https://doi.org/10.1029/2009JD013574).
- , and —, 2011: Observed evidence of an impact of the Antarctic sea ice dipole on the Antarctic Oscillation. *J. Climate*, **24**, 4508–4518, doi:[10.1175/2011JCLI3965.1](https://doi.org/10.1175/2011JCLI3965.1).
- , H. Hu, and L. Zhang, 2011: Observed influences of autumn–early winter Eurasian snow cover anomalies on the hemispheric PNA-like variability in winter. *J. Climate*, **24**, 2017–2023, doi:[10.1175/2011JCLI4236.1](https://doi.org/10.1175/2011JCLI4236.1).
- Wu, Z., J. Li, B. Wang, and X. Liu, 2009: Can the Southern Hemisphere annular mode affect China winter monsoon? *J. Geophys. Res.*, **114**, D11107, doi:[10.1029/2008JD011501](https://doi.org/10.1029/2008JD011501).
- Xue, F., H. Wang, and J. He, 2003: Interannual variability of Mascarene high and Australian high and their influences on summer rainfall over East Asia. *Chin. Sci. Bull.*, **48**, 492–497, doi:[10.1007/BF03183258](https://doi.org/10.1007/BF03183258).
- Yu, L., R. A. Weller, and B. Sun, 2004: Improving latent and sensible heat flux estimates for the Atlantic Ocean (1988–99) by a synthesis approach. *J. Climate*, **17**, 373–393, doi:[10.1175/1520-0442\(2004\)017<0373:ILASHF>2.0.CO;2](https://doi.org/10.1175/1520-0442(2004)017<0373:ILASHF>2.0.CO;2).
- , X. Jin, and R. A. Weller, 2006: Role of net surface heat flux in seasonal variations of sea surface temperature in the tropical Atlantic Ocean. *J. Climate*, **19**, 6153–6169, doi:[10.1175/JCLI3970.1](https://doi.org/10.1175/JCLI3970.1).
- , —, and —, 2008: Multidecade global flux datasets from the Objectively Analyzed Air–Sea Fluxes (OAFlux) project: Latent and sensible heat fluxes, ocean evaporation, and related surface meteorological variables. OAFlux Project Tech. Rep. OA-2008-01, Woods Hole Oceanographic Institution, 64 pp.
- Yue, X., and H. Wang, 2008: The springtime North Asia cyclone activity index and the southern annular mode. *Adv. Atmos. Sci.*, **25**, 673–679, doi:[10.1007/s00376-008-0673-5](https://doi.org/10.1007/s00376-008-0673-5).
- Zheng, F., and J. Li, 2012: Impact of preceding boreal winter southern hemisphere annular mode on spring precipitation over south China and related mechanism (in Chinese). *Chin. J. Geophys.*, **55**, 3542–3557.
- , —, R. T. Clark, R. Q. Ding, F. Li, and L. Wang, 2015: Influence of the boreal spring southern annular mode on summer surface air temperature over northeast China. *Atmos. Sci. Lett.*, **16**, 155–161, doi:[10.1002/asl2.541](https://doi.org/10.1002/asl2.541).